

Dissecting interactions between root-knot nematode effectors and lipid signaling involved in plant defense

Brown Horowitz , S. Agricultural Research Organization

Elling, A. Washington State University WA

Davis, E.L. North Carolina State University NC

Project award year: 2014

Three year research project

Root-knot nematodes, *Meloidogyne* spp., are extremely destructive pathogens with a cosmopolitan distribution and a host range that affects most crops. Safety and environmental concerns related to the toxicity of nematicides along with a lack of natural resistance sources threaten most crops in Israel and the U.S. This emphasizes the need to identify genes and signal mechanisms that could provide novel nematode control tactics and resistance breeding targets. The sedentary root-knot nematode (RKN) *Meloidogyne* spp. secrete effectors in a spatial and temporal manner to interfere with and mimic multiple physiological and morphological mechanisms, leading to modifications and reprogramming of the host cells' functions, resulted in construction and maintenance of nematodes' feeding sites. For successful parasitism, many effectors act as immunomodulators, aimed to manipulate and suppress immune defense signaling triggered upon nematode invasion. Plant development and defense rely mainly on hormone regulation. Herein, a metabolomic profiling of oxylipins and hormones composition of tomato roots were performed using LC-MS/MS, indicating a fluctuation in oxylipins profile in a compatible interaction. Moreover, further attention was given to uncover the implication of WRKYs transcription factors in regulating nematode development. In addition, in order to identify genes that might interact with the lipidomic defense pathway induced by oxylipins, a RNAseq was performed by exposing *M. javanica* second-stage juveniles to tomato protoplast, 9-HOT and 13-KOD oxylipins. This transcriptome generated a total of 4682 differentially expressed genes (DEGs). Being interested in effectors, we seek for DEGs carrying a predicted secretion signal peptide. Among the DEGs including signal peptide, several had homology with known effectors in other nematode species, other unknown potentially secreted proteins may have a role as root-knot nematodes' effectors which might interact with lipid signaling. The molecular interaction of LOX proteins with the Cyst nematode effectors illustrate the nematode strategy in manipulating plant lipid signals. The function of several other effectors in manipulating plant defense signals, as well as lipids signals, weakening cell walls, attenuating feeding site function and development are still being studied in depth for several novel effectors. As direct outcome of this project, the accumulating findings will be utilized to improve our understanding of the mechanisms governing critical life-cycle phases of the parasitic *M. incognita* RKN, thereby facilitating design of effective controls based on perturbation of nematode behavior—without producing harmful side effects. The knowledge from this study will promote genome editing strategies aimed at developing nematode resistance in tomato and other nematode-susceptible crop species in Israel and the United States.

Summary Sheet

Publication Summary

PubType	IS only	Joint	US only
Abstract - Presentation	3	1	0
Book Chapter	0	1	0
Reviewed	1	0	0

Training Summary

Trainee Type	Last Name	First Name	Institution	Country
Ph.D. Student	Fitoussi	Natalia	ARO Volcani Center	Israel
Postdoctoral Fellow	Zhang	Lei	NCS	USA
Postdoctoral Fellow	Chinnapandi	Bharathiraja	Volcani Center	Israel

Contribution of Collaboration. During the life time of this grant the investigators met during April 2016 in Israel, April 2018 in Israel and July 2018 in US to discuss the project and future collaboration and were pleased with progress according the time outline set for this project.. Manuscripts based on the achieved data regards WRKYs have been published and differential expressed genes encoding for various effectors related to fatty acids signals will be co-authored by the US and IS researchers. During the duration of the current research the US lab focused on studying the role of 2G02-AtGST16 interaction in the oxylipin or jasmonate pathway during RKN infection. The effect of overexpressing 2G02 on plant response was evaluated through RNAi targeting 2G02 and analyzing T-DNA mutant of Arabidopsis AtGST16. Furthermore, this plant material was tested for altered expression of marker genes of plant oxylipin pathway, and accumulation of intermediates or end products of oxylipin pathway without or under RKN infection, in order to study how 2G02 may modulate lipid signaling-mediate plant defense response for successful parasitism. The system we designed which include monitoring of marker gene expression of salicylic acid-based lipid signaling including *PR1*, *PR2*, and *PR5* and for the jasmonate signaling pathway we markers for *PR3*, *PR4*, *AOS*, *AOC3*, *AOC4*, and *OPR3* following overexpression of *M. incognita* or *M. javanica* effectors proved as a reliable method to identify effectors implicated in lipid signals regulation. The first group of effectors chosen for transient expression in *N. benthamiana* include Hs2A05, Mi10A06, Hs30C02, Mi5G05, Mi7H08, Mi8D05, Mi9H10, Mi16D10, Mi35F03, Mi2G06B, Mi6D09B. Each of these effectors has some additional phenotypic data to compare to response in the transient expression system to corroborate the utility of the system to identify root-knot nematode effectors that affect plant lipid signaling pathways. The implication of other effectors derived by the IS group following RNAseq of *M. javanica* J2s following exposure to 9-HOT was discussed with the US group and will yield future collaboration. Moreover the methodology developed by the US group will be further used to identify nematode effectors interact withplant WRKYs genes which have shown as ultimate candidates regulating parasitism by the RKN.

ACHIEVEMENTS

Evaluation of the research achievements as related to the original research proposal and objectives. The current research entitled: "Dissecting interaction between Root-Knot Nematodes Effectors and Lipid Signaling Involved in Plant Defense" is aimed at analyzing the molecular interactions between the root-knot nematode effectors and defense signaling pathways in plants, using tomato and/or Arabidopsis as a model host. The overall objectives that were originally placed include i) determining the role of nematode Fatty acid and Retinol (FAR) proteins in interfering with intracellular plant signaling related to host defenses, ii) functionally characterize interactions between root knot nematode effector genes and the plant signaling pathway and iii) study the role of fatty acids pathway genes in the root knot nematode infection process. During the life time of this research both the US and the IS groups have been fully engaged with generating new data concerning gene networks and pathways that determine plant response to nematode infection in relation to fatty acids signals. The IS group has focused on tomato plants infected with *Meloidogyne javanica* while the US lab has focused on Arabidopsis plants infected with *Heterodera Schachtii* as well as Arabidopsis infected with *Meloidogyne incognita*. Altogether our findings further illustrate the implication of lipid signals in regulating RKN disease in their host plant. The research achievements related to the mentioned goals will be elaborated for each research group and their significance will be further discussed.

Functionally characterize interactions between nematodes effectors and plant FA-related genes. The US lab was able to confirm the localization of AtLOX1 and Hs2A05 (VAP2 effector) within the cytoplasm of plant cells using GFP labeled proteins in an *N. benthamiana* leaf transient expression assay (Fig. 1). Our preliminary studies had discovered

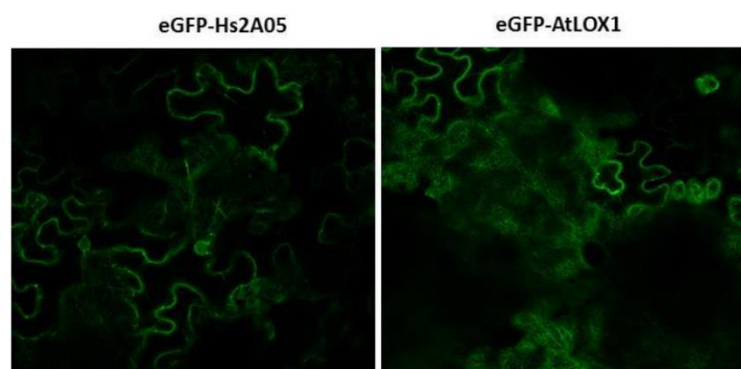


Fig. 1. The 2A05 effector and plant AtLOX1 protein both localize to the cytoplasm of plant cells using GFP labeled proteins. The direct interaction of the 2A05 effector and AtLOX1 proteins within plant cells, however, was not confirmed by BiFC assays.

that the soybean cyst nematode effector Hg2A05, a venom allergen-related effector protein (VAP2) interacts with a plant lipoxygenase (LOX1) in yeast two-hybrid (Y2H) screening using cDNA libraries prepared from roots of Arabidopsis or soybean plants. The specific

interaction between 2A05 and Arabidopsis AtLOX1 was further confirmed by co-transformation test of Y2H but was not confirmed within plant cells using bifluorescence complementation (BiFC) assays. We then screened about 30 root-knot nematode *M. incognita* effector tested with the target plant LOX proteins including AtLOX1, AtLOX3 and AtLOX4 using yeast two-hybrid analyses but did not identify interaction of any RKN effector tested with the target plant LOX proteins. We chose to conduct yeast two-hybrid screens of individuals RKN effectors against a full Arabidopsis root cDNA library to identify potential host target proteins (beyond LOX) that interact with RKN effectors. These proteins-protein interaction screens are slow and cumbersome and have identified few candidates that may be involved in host cell lipid signaling. We have discovered that the root-knot nematode *M. incognita* effector 2GO2 interacts with a plant glutathione S-transferase (AtGST16, At2G02930) in yeast two-hybrid screening using cDNA libraries prepared from roots of Arabidopsis plants infected by *M. incognita* (Fig. 2). Previous studies had shown that glutathione metabolism is important for successful RKN parasitism (Baldacci-Cresp et al. 2012). GSTs were extensively studied for their roles in detoxification in plants, but some GSTs had been shown to be involved in stress responses (Marrs 1996). Specifically, the AtGST16 had been shown to be involved in plant defense against fungal pathogens (Hok et al. 2011, Lee et al. 2007). We will investigate the role of the interaction between 2GO2 and AtGST16 in plant oxylipin/jasmonate pathway or other defense pathways during RKN infection. We have recently been able to confirm the direct interaction of Mi2GO2 and AtGST16 within host plant cells by BiFC in the *N. benthamiana* leaf transient expression system (Fig. 2).

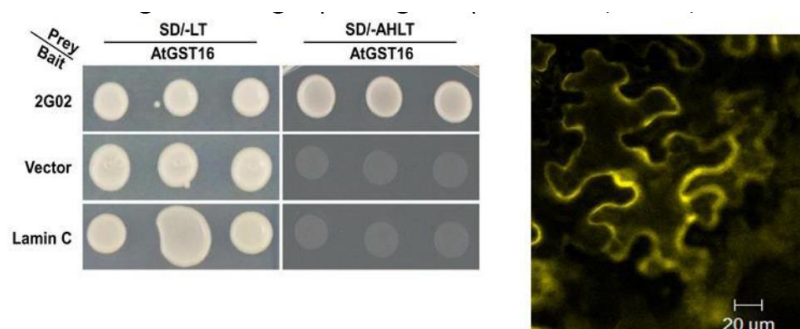


Fig. 2. *M. incognita* effector 2GO2 interacts with AtGST16. (Left) Yeast two-hybrid assay where the Mi2GO2 effector without signal peptide-encoding sequence was cloned into bait vector pGBKT and AtGST16 was cloned into prey vector pGADT. C-transformation of the two plasmids into yeast strain AH109 led to activation of reporter genes and growth of yeast on SD/-Ade/-His/-Leu/-Trp selection media (SD/-AHLT). Control vectors (vector and Lamin C) were used to confirm the specific interaction between 2GO2 and AtGST16. (Right) The direct interaction of Mi2GO2 and AtGST16 were confirmed within leaf cells of *N. benthamiana* using the BiFC assay.

Next according to goal no. 2 the US group made a significant progress in analyzing five known nematode effectors (Table 1) for their ability to influence expression of plant genes encoding pathogenesis-related (PR) proteins or known members of plant lipid signaling pathways (Table 3).

Table 1. Nematode effector protein genes expressed in *N. benthamiana*.

Gene Construct	Accession #	RKN or SCN
2G02	AF531161	RKN
7H08	AF531168	RKN
8D05	HQ728271	RKN
9H10	AF531167	RKN
30C02	JF896103	SCN
pEarlyGate201*		N/A

*Empty vector control.

Table 3. Real Time QPCR Primers for Plant defense Genes

Gene Name	Host	Accession #	Primer	Sequence
Elongation factor-1 α (NbEF1 α)	NB	AY206004.1	NbEF1 α -QPCR-F	GACCACTGAAGTTGGATCTGTTG
			NbEF1 α -QPCR-R	TAGCACCAGTTGGGTCCTTCTT
Protein phosphatase 2A (PP2A)	NT	TC21939	PP2A-QPCR-F	GACCCTGATGTTGATGTTTCGCT
			PP2A-QPCR-R	GAGGGATTTGAAGAGAGATTTC
PR1	NB	JN247448.1	NbPR1-FP	GGTCAATACGGCGAAAACCT
			NbPR1-RP	ACCCTAGCACATCCAACACG
PR2	NT	M60460.1	NbPR2-QPCR-242-F	ATTTGTTGCTCCTGCCATGC
			NbPR2-QPCR-363-R	CTTTGGCGGGTTGGTATTC
OPR3	NB	CN745683.1	NbOPR3-QPCR-188-F	TGGCCAAACAGAGGCAGGTA
			NbOPR3-QPCR-325-R	TGTGCCACAGCCTCAATTCC
PR5	NB	AF154636.1	NbPR5-QPCR-27-F	TTGGATGAGAGCCAGAACAAGC
			NbPR5-QPCR-145-R	GCATGGTGGATTGACTTAGCC
PAL5	NT	EB684217.1	NbPAL5-FP	ACGTCTTTGCTTACGCTGAT
			NbPAL5-RP	CGTGATTCTTGCACTCTCGA
Epi-aristolochene dihydroxylase (EAH)	NB	KM410159.2	NbEAH-QPCR-F-161	ACCACGTCCTTAGAGATTTAGC
			NbEAH-QPCR-R-259	TGCCATGTCCCTAGAAGTAACC
Sesquiterpene synthase (TPS1)	NB	KF990999.1	NbTPS1-QPCR-F-149	AGGAACAAACGAGGAGTATGC
			NbTPS1-QPCR-R-249	AAGTGGTAGGATATGCCAAGG

A transient system to express individual nematode effectors in leaves of *Nicotiana benthamiana* was adopted to use quantitative real-time RT-PCR to assess target plant gene expression in time-course assays from 1-4 days after expression of the nematode effector genes.

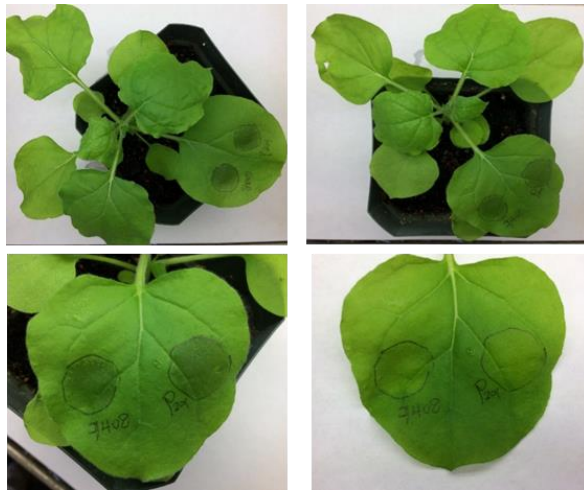


Fig. 3. This *N. benthamiana* leaf has been infiltrated with two agro solution strains with one GOI (7H08 or 8D05) and the empty vector (PEarleyGate 201).

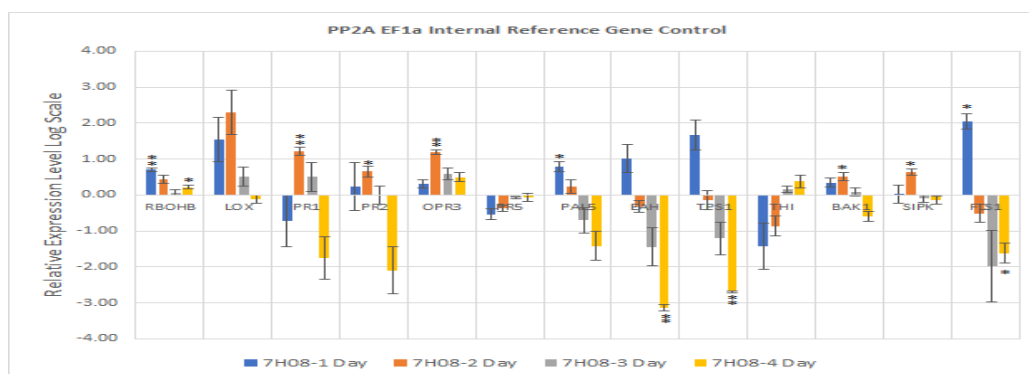


Figure 1. Time-course analysis of pathogenesis-related (PR) gene expression by qPCR of *N. benthamiana* leaves infiltrated with 7H08 at 1 (blue), 2 (orange), 3 (grey), and 4 (yellow) days post infiltration. The presented data are the mean fold changes and standard errors in PR transcript levels relative to leaf tissue infiltrated with an empty vector control from three biological replicates. An asterisk (*) indicates that the mean fold change is significantly different from 0.0 as determined by t-test (* $P < 0.05$, ** $P < 0.01$).

Of the genes tested, the **7H08** nematode effector gene showed relatively consistent, statistically significance (paired t-test, $p=.05$), and highest relative fold-change in target gene expression results (**Figure 1**). 7H08 infiltrated leaf tissue showed significant results particularly looking at the expression levels of PR genes EAH, TPS1, and FLS2 (**Figure 1**). Levels of EAH and TPS1 on day 4 were both found to be down-regulated ~3 fold in comparison to the empty vector control. FLS2 was found to be upregulated approximately ~2 fold on day 1 and down-regulated ~1.5 fold on day 4. The overall results of 7H08 nematode effector expression suggest relatively rapid response of plant PR and lipid-signaling pathways with downregulation of plant response after 48 hours of 7H08 effector expression.

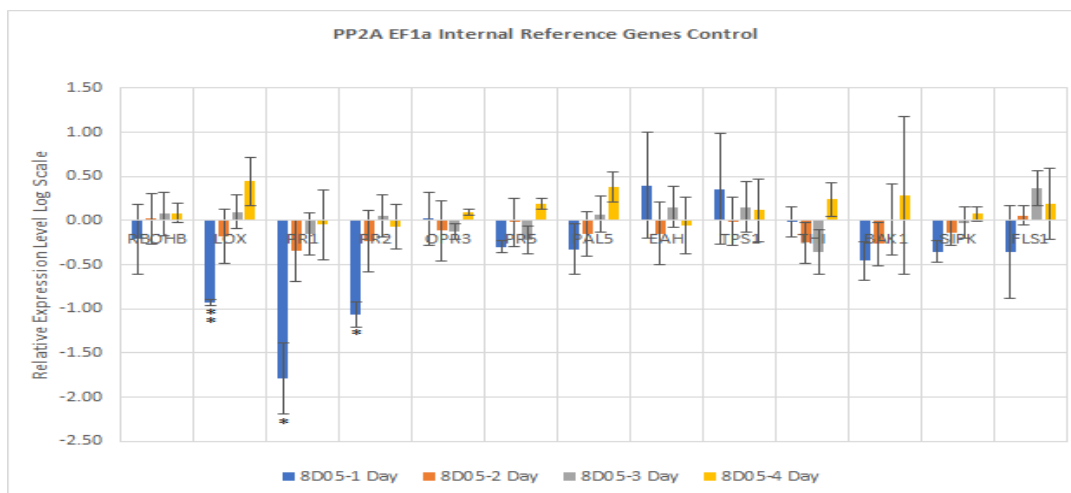


Figure 2. Time-course analysis of pathogenesis-related (PR) gene expression by qPCR of *N. benthamiana* leaves infiltrated with 8D05 at 1 (blue), 2 (orange), 3 (grey), and 4 (yellow) days post infiltration. The presented data are the mean fold changes and standard errors in PR transcript levels relative to leaf tissue infiltrated with an empty vector control from three biological replicates.

Plant target gene response to expression of the 8D05 nematode effector gene was the inverse of that observed with the 7H08 effector (Figure 2). Rapid downregulation of the target plant genes was observed by 24 hours after 8D05 effector expression, with significant downregulation of plant LOX, PR1, and PR2 gene expression in the early response.

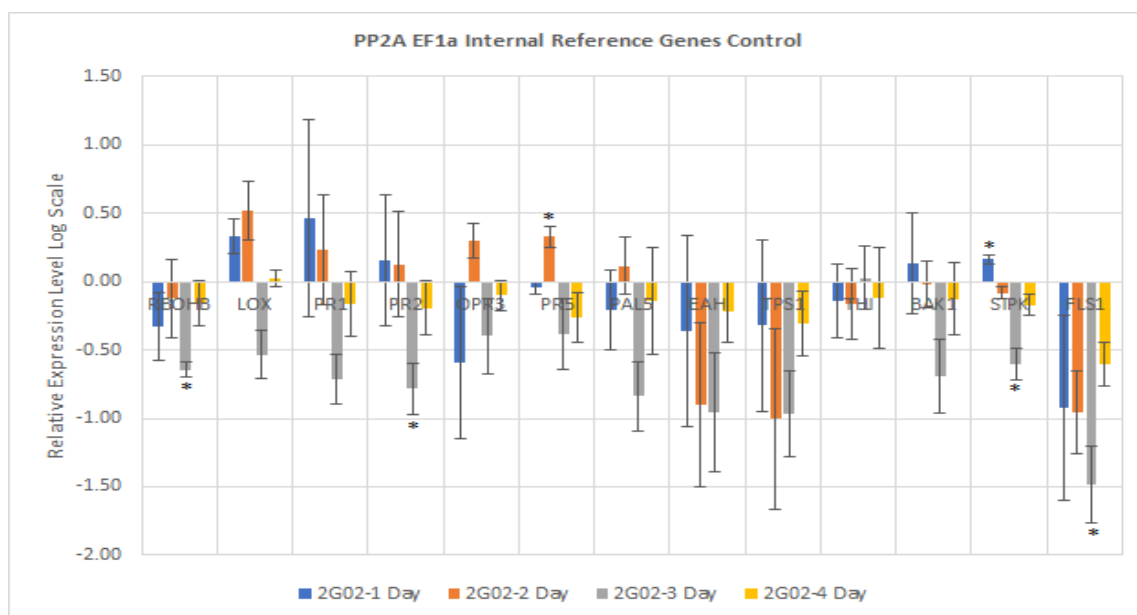


Figure 3. Time-course analysis of pathogenesis-related (PR) gene expression by qPCR of *N. benthamiana* leaves infiltrated with 2G02 at 1 (blue), 2 (orange), 3 (grey), and 4 (yellow) days post infiltration. The presented data are the mean fold changes and standard errors in PR transcript levels relative to leaf tissue infiltrated with an empty vector control from three biological replicates

Expression of the nematode **2G02** effector gene induced downregulation of the majority of target plant genes, especially after 48 hours of nematode effector expression. The overall fold-change was relatively low, but significant downregulation of plant RBOHB, PR2, and FLS1 were observed by 72 hours after 2Go2 effector expression in leaves. Significant increases in expression of PR5 by 48 hours and SIPK within 24 hours were observed upon 2G02 expression, but the relative fold-change was minimal.

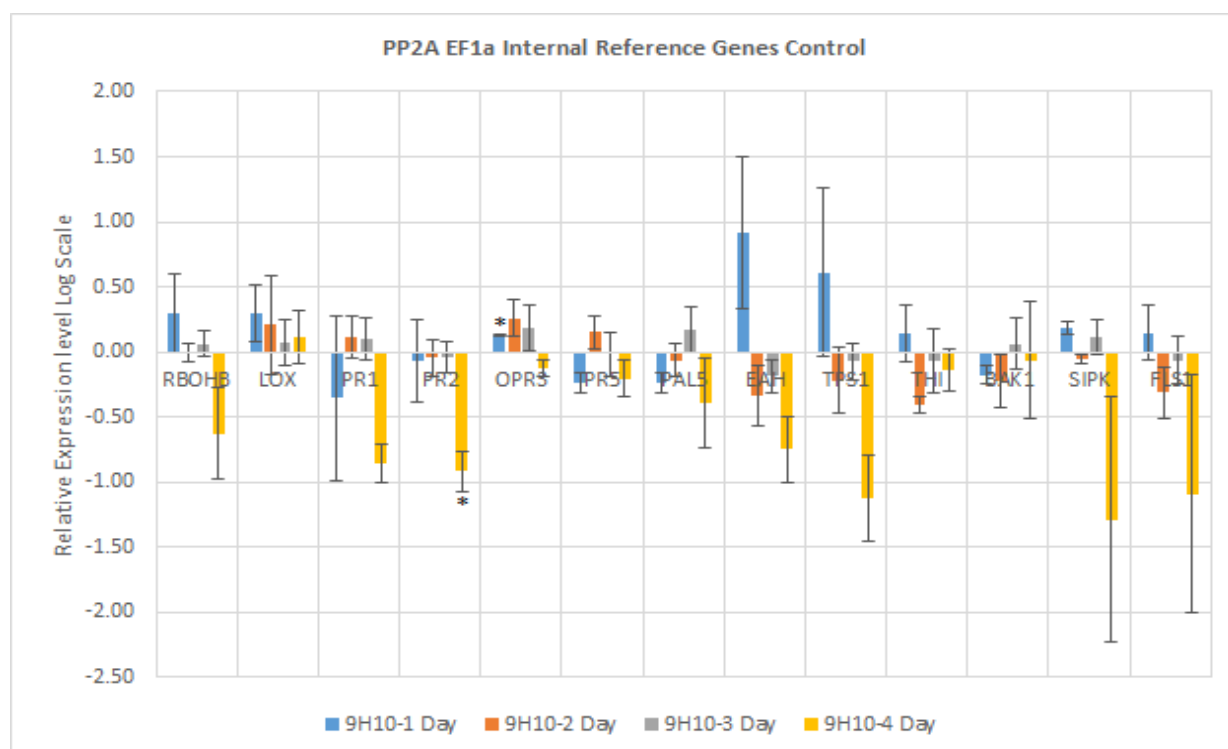


Figure 4. Time-course analysis of pathogenesis-related (PR) gene expression by qPCR of *N. benthamiana* leaves infiltrated with 9H10 at 1 (blue), 2 (orange), 3 (grey), and 4 (yellow) days post infiltration. The presented data are the mean fold changes and standard errors in PR transcript levels relative to leaf tissue infiltrated with an empty vector control from three biological replicates.

Expression of the **9H10** nematode effector gene provided a mixture of increase in expression of some target plant genes early in the response (within 48 hours) and downregulated later in the plant response (after 72 hours). While expression the OPR5 plant gene was significantly increased by 24 hours after 9H10 expression, the fold-change was very low. Downregulation of most plant target genes by 96 hours after 9H10 effector expression was the only relatively clear pattern of plant response to the 9H10 effector.

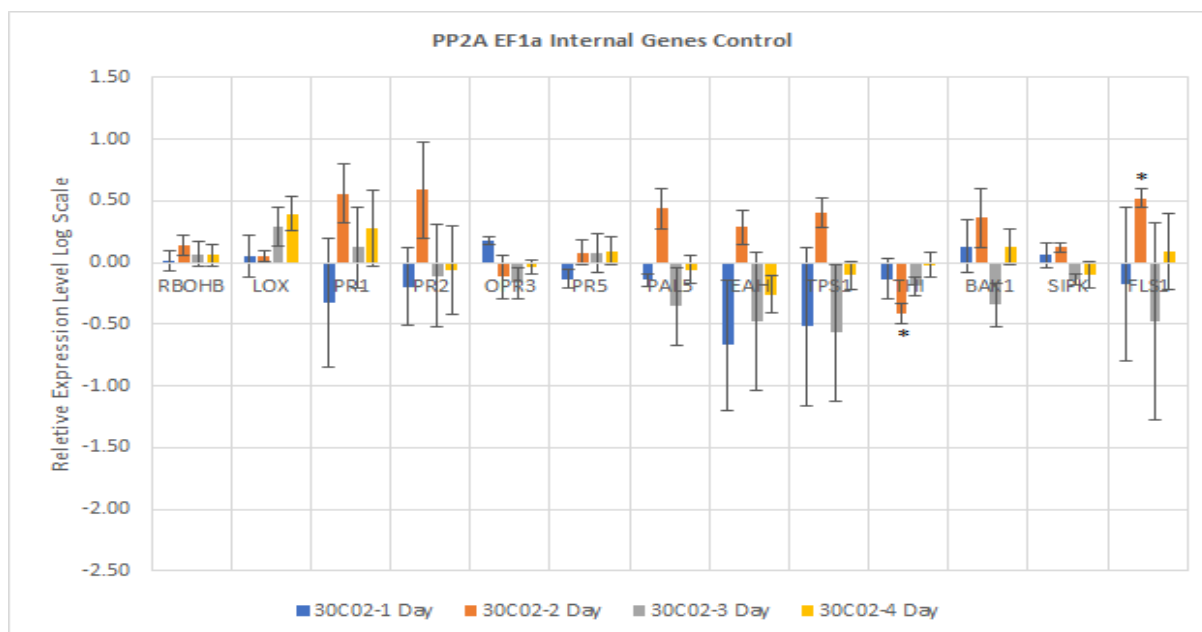


Figure 5. Time-course analysis of pathogenesis-related (PR) gene expression by qPCR of *N. benthamiana* leaves infiltrated with 30C02 at 1 (blue), 2 (orange), 3 (grey), and 4 (yellow) days post infiltration. The presented data are the mean fold changes and standard errors in PR transcript levels relative to leaf tissue infiltrated with an empty vector control from three biological replicates.

Expression of the **30C02** nematode effector gene induced downregulation of a subset of target plant genes within 24 hours and a relatively rapid reversion to increased expression of these same plant target genes by 48 hours after 30C02 effector expression. 30C02 was the only nematode effector analyzed that induced this relatively rapid reversion of plant gene expression from initial downregulation to increased expression by 48 hours after effector expression.

Uncovering signaling networks regulating RKN disease. Major achievements gained by the IS group will be outlined. Our preliminary data of tomato RNA-seq have placed the WRKYs group of transcription factor as an important transcription factor family which might have a determinant role in regulating plant defense response. WRKY transcription factors are one of the largest gene families for transcriptional regulators in plants and form essential parts of different signaling pathways that modulate many processes, including plant defense as reviewed by Euglem, Pandey and Rushton (Eulgem et al. 2000, Pandey and Somssich 2009,

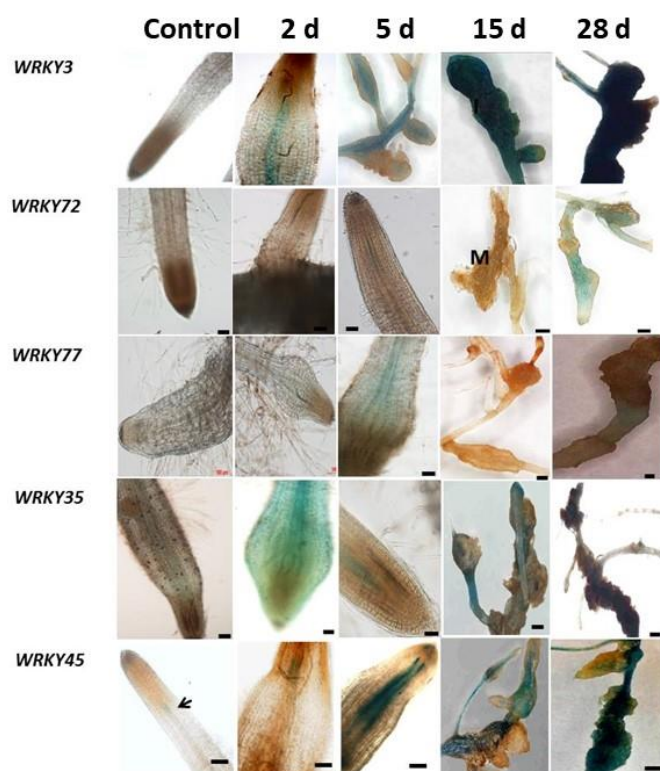


Figure 3. Microscopic analysis of β -glucuronidase (GUS) expression patterns in root-knot nematode (RKN)-infected tomato roots harboring the *SIWRKY3*, *SIWRKY72*, *SIWRKY77* and *SIWRKY35* promoter-GUS fusion constructs. For each *SIWRKY*:GUS line noninoculated and inoculated at 2, 5, 15 and 28 dai root samples were taken for GUS bioassay.

Rushton et al. 2010). Among these group candidate transcripts derived from RNAseq analysis (Iberkleid et al. 2015) were evaluated for their potential as a target for nematode effectors which are being extensively studied by the US group. During the life time of the current research significant evidence were achieved for the involvement of several WRKYs gene among them *SIWRKY3*, *SIWRKY35*, *SIWRKY72*, *SIWRKY77* and *SIWRKY45* in regulating plant response to nematodes. GUS reporter lines generated for each of the respective genes indicated these genes are induced upon nematode infection, with *SIWRKY3* and *SIWRKY45* demonstrating high

expression upon infection (Fig. 3). High induction of *SIWRKY3* and *SIWRKY45* pave the way for function

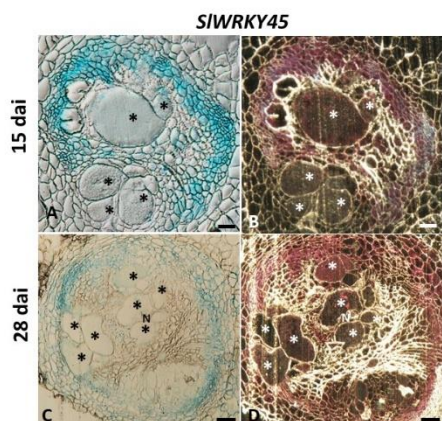
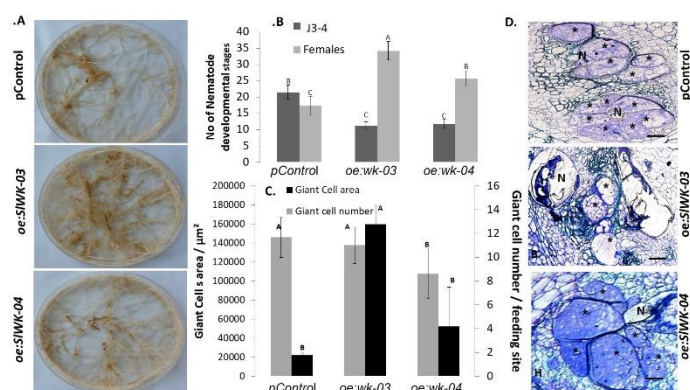


Figure 4. Activity of WRKY45 promoter within thin sections of galls analyzed by GUS staining in representative transformed tomato lines infected with *Meloidogyne javanica*. Microscopic analyses of β -glucuronidase (GUS) activity in cross-sections of tomato root gall expressing WRKY45 promoter-GUS constructs at 15 and 28 dai. At 15 and 28 dai all observed giant cells were already mature. ((A, B) Galls sections induced on WRKY45:GUS line at 15 dai. (C, D) Galls sections induced on WRKY45:GUS line at 28 dai. (N) The female body of the nematode can be seen at the edge of the giant cells (*). Bars, 200 μ m. GUS staining is observed as blue color in whole mounts, and as a red precipitate in the dark field micrographs of the sections.

analyze the role of both genes through continuous study.

Thin sections analysis demonstrate SIWRKY45 is highly expressed within feeding sites both at 15 and 28 dai (Fig. 4). Function analyzing the role of SIWRKY45 have placed this WRKY



candidate as a potential target for nematode, as tomato roots overexpressing WRKY45 support nematode development as illustrated by increased number of females observed on transgenic roots overexpressing SIWRKY45

Fig. 5. Overexpression of *SIWRKY45* in tomato hairy roots promote RKN *M. javanica* nematode development . A. Increased susceptibility of tomato hairy roots expressing *SIWRKY45* (*oe:wk-03*, *oe:wk-04*) is accompanied by increased galling occurrence compared with pControl line. **B.** Meloidogyne susceptibility/resistance of vector transformed roots and transgenic tomato roots expressing *WRKY45* compared with pControl line. All roots lines were inoculated with 300 sterile pre-parasitic J2s were assessed for J3-4 juveniles and mature females development at 28 dai through observation under the dissecting microscope following staining with acid fuchsin dye. Note the significant ($P < 0.05$) increase in percentage of mature females in *oe:wk-03* and *oe:wk-04* in comparison with vector control roots. Data are expressed as means of 25 plants from each line; the experiment was repeated three times, giving consistent results. The percentage of each developmental stage is represented by a mean standard error. Different letters above the bars denote a significant difference ($P \leq 0.05$, analysis of variance) between hairy roots lines analyzed by Tukey-Kramer multiple comparison tests. **C.** Longitudinal sections of *Meloidogyne javanica* feeding sites developed in root lines *oe:wk-03*, *oe:wk-04* and pControl . Average GC area was measured on 50 GC systems and average number of GCs of each feeding site system as measured on 60 gall cross sections for each root line and measurements are given as mean \pm standard error. Different letters above the bars denote statistically significant differences ($P \leq 0.05$, analysis of variance) determined by Tukey-Kramer multiple comparison tests. Giant-cell (GC) area of plants carrying the *SIWRKY45* gene were more extensive compared with pControl line. **D.** Thin sections of *oe:wk-03*, *oe:wk-04* and control line were stained with toluidine blue; * = GC, N = nematode, bar = 100 μ m.

(Fig. 5). In the next step we evaluate the contributions of biosynthesis and regulation of hormones, including JA, SA, BA, and IAA, to the observed increased susceptibility of *oe:wk-03*- and *oe:wk-04*-overexpressing roots, expression of a set of gene markers involved in these various pathways was investigated by means of qRT-PCR. Transcription of genes whose induction patterns are often used as molecular markers for the activation of the SA signaling pathways were analyzed; as pathogenesis-related (PR-1; accession no. M69247) and phenylalanine ammonia lyase (PAL5; accession no. M90692.1). Although no differences between PAL5 expression in pControl and *oe:wk-03*-infected lines were observed, a significant decrease was observed in PR-1 expression in the *oe:wk-03*-infected line compared with the pControl line (Fig. 6). The expression of the JA biosynthesis genes OPR (accession no. A1486721) did not show any changes in its profile, whereas the JA marker gene proteinase inhibitor II (Pin2; accession no. L21194) clearly exhibited repression in *oe:wk-03* compared with pControl, following infection. Next, the cytokinin response factors (CRFs) – part of the cytokinin signal transduction pathway – were analyzed. Both CRF1 (accession no. NM001247062) and CRF6 (accession no. XM004241080) have been downregulated in *oe:wk-03* compared with pControl, following

infection, which suggests suppression of the cytokinin signaling pathway in the overexpressing infected line (Fig. 6).

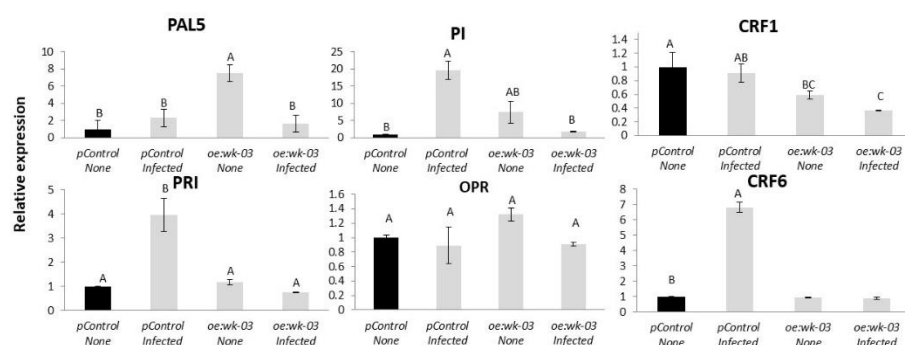


Figure 6. Analyzing the effect of WRKY45 overexpression in manipulating hormonal pathways response. Expression level of defense-related target genes in *oe:wk-03* expressing root line compared with vector control prior and 5 DAI with *Meloidogyne javanica*. Total RNA was prepared from pControl transformed control roots and roots expressing *SIWRKY45* with/without infection. The graph shows the mean and standard error of the relative amount of transcripts of these genes in *SIWRKY45* expressing roots (*oe:wk-03*) in comparison with vector transformed control roots (pControl) growing under the same conditions (vector control expression level set at zero). All target genes were normalized using the normalization factor calculated as the geometric mean of the expression levels of three tomato endogenous reference genes 18S, β -actin and β -tubulin. Each reaction was performed in triplicate and the results represented the mean of two independent biological replicates. Statistical significance of the differences between *oe:wk-03* and pControl transformed control roots were determined by Tukey-Kramer multiple comparison test, and significant differential expression ($P \leq 0.05$) is indicated with asterisks. The experiments were repeated three times with similar results.

As *SIWRKY3* expression was the most responsive to nematode (Fig. 3), its role in nematode infection was further explored with overexpression and genetic knockout tools. Plant binary vector containing the 1383-bp *SIWRKY3* open reading frame under the control of the CaMV

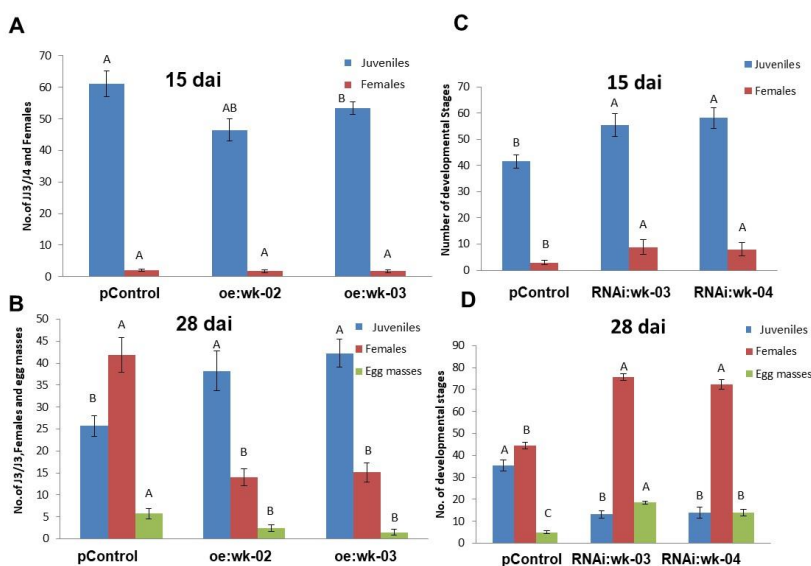


Figure 7. Overexpression of *SIWRKY3* in tomato roots increases root susceptibility to infection by the root-knot nematode *M. javanica*. *Meloidogyne* susceptibility/resistance of transgenic tomato roots overexpressing *SIWRKY3* (*oe*) (A, B) and transgenic roots expressing *WRKY3* dsRNA (*RNAi*) (C, D) was measured as nematode developmental stages counted at 15 and 28 dai in comparison to the pControl line. All root lines were inoculated with 300 sterile parasitic J2s and the infected roots were assessed for development of J3/J4s and mature females at 15 (A, C) and 28 (B, D) dai for each root line, through observation under the dissecting microscope following staining with acid fuchsin dye. Data are expressed as means of 25 plants from each line; the experiment was repeated three times, giving consistent results. The percentage of each developmental stage is represented by a mean standard error. Different letters above the bars denote a significant difference ($P \leq 0.05$, analysis of variance) between hairy root lines analyzed by Tukey-Kramer multiple comparison tests.

selective media. Similarly, *SIWRKY3* RNAi-silenced lines were generated by amplifying a

571-bp product and were further subcloned in pHANNIBAL vector, (Wesley et al. 2001) generating the hairpin dsRNA complementary to *SIWRKY3*, under the constitutive CaMV 35S promoter, followed by cloning into the binary vector pART27 which was used for *A. rhizogenes*-mediated transformation. To determine the effect of *SIWRKY3* overexpression on disease development in tomato, hairy roots from transgenic and pControl roots (carrying pART27) were inoculated with *M. javanica* J2s, and nematode developmental stages were monitored at 15 and 28 dai (Fig. 7A and B). Remarkably, *SIWRKY3* overexpression resulted in an increased number of juveniles at 28 dai, however, there was a dramatic decrease of nematodes molting to the female stage and associated number of egg masses recovered (Fig. 7B). In sharp contrast, silencing of *SIWRKY3* reduced the number of J2s but increased the number of females and egg masses, at 28 dai (Fig. 7D). Taken together, these data provide evidence that *SIWRKY3* is a major player in controlling the development, reproduction, and performance of RKN.

***SIWRKY3* overexpression regulates oxylipin- and hormone-biosynthesis during early RKN infection processes.** To begin to understand the mechanisms downstream of *SIWRKY3*-mediated host responses to RKN, targeted metabolite analysis was performed to investigate phytohormone and oxylipin—oxygenated fatty acids involved in defense responses against pathogens—and related metabolites were measured in the *WRKY3*-overexpressing line at 5 and 15 dai using LC–MS/MS analysis (Figs. 8, 9). Accumulation of key metabolites of the shikimate pathway was observed, e.g., increased accumulation of cinnamic acid (CA)—a phenylpropanoid with antioxidant activity—was observed in roots overexpressing *SIWRKY3* at 5 dai. The accumulation of shikimate-derived benzoates also

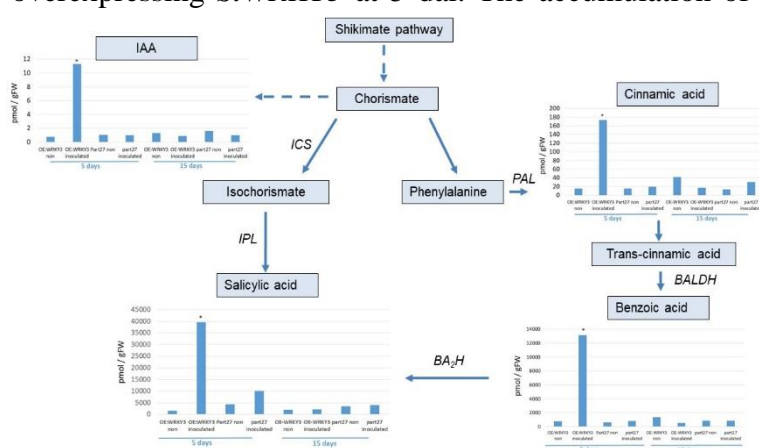


Figure 8. Analysis of major branch-point intermediates and products associated with and derived from the shikimate pathway. Changes in levels of the metabolites: cinnamic acid, benzoic acid, salicylic acid and indole-3-acetic acid (IAA) were measured through direct LC–MS/MS analysis in negative-phase mode in root tissues at 5 and 15 dai with *M. javanica* J2s, and data were expressed as means of four replicates. Mock treatments consisted of inoculation with H₂O only. Errors bars correspond to SD (n = 4), and different letters above the bars denote a significant difference ($P < 0.05$, analysis of variance) between samples, as analyzed by Tukey–Kramer multiple comparison test.

increased in the *SIWRKY3*-overexpressing line, as well as that of the converted metabolite SA resulting from the activity of benzoic acid 2-hydroxylase. The level of the phytohormone IAA also increased in roots overexpressing *SIWRKY3* at 5 dai (Fig. 8). Oxylipins of the reductase pathways, the hydroxy fatty acids 13-hydroxy octadecadienoic acid

(13HOD), 13-hydroxy octadecatrienoic acid (13HOT), 9-hydroxy octadecadienoic acid (9HOD) and 9-hydroxy octadecatrienoic acid (9HOT), were significantly increased 5 dai in the *SlWRKY3*-overexpressing line compared to pControl lines, with no significant differences at 15 dai (Fig. 9). In addition, a significant increase in the accumulation of 12, 13-epoxy-metabolites generated through the cytochrome p450 pathway was observed in roots overexpressing *SlWRKY3* at 5 dai, including epoxyoctamonoenoic acid (12,13-EpOM), 12,13-epoxyoctadecadienoic acid (12,13-EpODE), and 12,13-dihydroxyoctadecenoic acid (12,13-DiHOM) diols resulting from conversion of the epoxy-metabolites by soluble epoxide

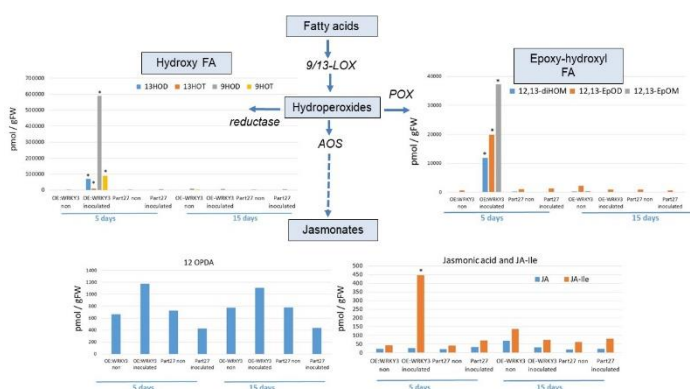


Figure 9. Analysis of products associated with and derived from the oxylipin pathway governed by lipoxygenase. Endogenous lipoxygenase (LOX), allene oxide synthase (AOS), and reductase and peroxygenase (POX)-derived oxylipins were analyzed. Oxylipin production was monitored by LC-MS/MS in negative-phase mode in root tissues at 5 and 15 dai with *M. javanica* J2s and data were expressed as the means of four replicates. Mock treatments consisted of inoculation with H₂O only. Errors bars correspond to standard deviation (n = 4), and different letters above the bars denote a significant difference ($P < 0.05$, analysis of variance) between samples, as analyzed by Tukey–Kramer multiple comparison test. FA, fatty acid.

hydrolase (sEH) (Fig. 9). Among the jasmonate group, significant differences were only observed for the bioactive isoleucine conjugate JA-Ile at 5 dai with concentrations increasing approximately 10-fold ($P < 0.05$) compared to pART27 control roots, with no significant differences observed for either JA or 12-OPDA (oxo-phytodienoic acid) (Fig. 9).

Research achievements related to goal no. 2 functionally characterize interactions between *M. javanica* effector genes and plant fatty acid pathways. During the first year we accomplished metabolic profile of oxylipins upon nematode infection of tomato through a collaboration with the lab of Prof Mochaël Kolomiets (College station, Texas A&M). To evaluate alteration of oxylipins-mediated defense pathways throughout tomato root infection by the RKN *M. javanica*, we performed a full characterization and identification profile of tomato roots oxylipins by harvesting inoculated roots at different time points: 5, 15 and 28 DAI, as well as noninoculated roots at the same time points to assess oxylipins changes accompanying nematode parasitism within roots. For that purpose, a comprehensive oxylipins metabolomics analysis was conducted by using LC-MS/MS platform, generating quantitative evaluation of approximately 100 oxylipins already identified through this system previously (Figure 10). Interestingly, for the majority of the tested oxylipins, inoculated root tissues exhibited a significant fluctuation of measured oxylipins throughout the time the

nematode is developing within root tissues, that is compared with noninoculated roots that generally exhibit no significant changes (Fig. 10).

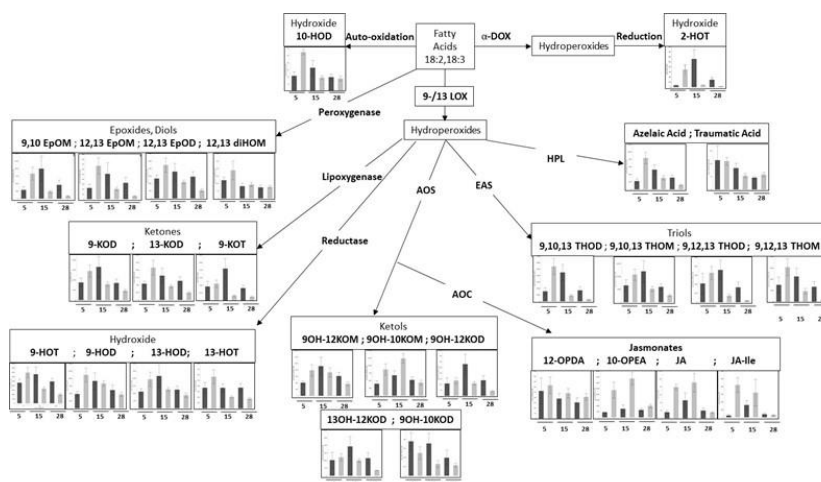


Figure 10. Integrated analysis of Tomato root galls' oxylipins pathway and profile, non-inoculated (dark grey) and inoculated (light grey) with *M.javanica* juveniles collected in different time points (5DAI, 15DAI and 28 DAI). Short names of oxylipins used in this scheme are: 18:2, Linoleic acid; 18:3, Linolenic acid; 2-HOT, 2(R)-Hydroxy-9(Z),12(Z),15(Z)-octadecatrienoic acid; 9,10,13 THOD, 9(S),12(S),13(S)-trihydroxy-10(E),15(Z)-octadecadienoic acid; 9,10,13 THOM, 9(S),12(S),13(S)-trihydroxy-10(E),15(Z)-octadecatrienoic acid; 9,12,13 THOD, 9(S),12(S),13(S)-Trihydroxy-10(E)-octadecenoic acid; 9,12,13 THOM, 9(S),12(S),13(S)-Trihydroxy-10(E),15(Z)-octadecadienoic acid; 12-OPDA, 12-Oxo-10,15(Z)-phytodienoic acid; 10-OPEA, 10-oxo-11-phytoenoic acid; JA, Jasmonic acid; JA-Ile, Jasmonic acid isoleucine; 9OH-12KOM, 9-hydroxy-12-oxo-octadecaenoic acid; 9OH-10KOM, 9-hydroxy-10-oxo-octadecaenoic acid; 9OH-12KOD, 9-hydroxy-12-oxo-octadecadienoic acid; 13OH-12KOD, 13-hydroxy12-oxo-octadecadienoic acid; 9OH-10KOD, 9-hydroxy-10-oxo-octadecadienoic acid; 9-HOT, 9(S)-Hydroxy-10(E),12(Z),15(Z)-octadecatrienoic acid; 9-HOD, 9(S)-Hydroxy-10(E),12(Z)-octadecadienoic acid; 13-HOD, 13(S)-Hydroxy-9(Z),11(E)-octadecadienoic acid; 13-HOT, 13(S)-Hydroxy-9(Z),11(E),15(Z)-octadecatrienoic acid; 9-KOD, 9-Keto-10(E),12(Z)-octadecadienoic acid; 13-KOD, 13-Keto-9(Z),11(E),15(Z)-octadecatrienoic acid; 9-KOT, 9-Keto-10(E),12(Z),15(Z)-octadecatrienoic acid; 9,10 EpOM, 9(R),10(S)-Epoxy-12(Z)-octadecenoic acid; 12,13 EpOM, 12(R),13(S)-Epoxy-9(Z)-octadecenoic acid; 12,13 EpOD, 11(S),12(S)-Epoxy-13(S)-hydroxy-9(Z),15(Z)-octadecadienoate; 12,13 diHOM, (±)-threo-12,13-Dihydroxy-9(Z)-octadecenoic acid, 10 HOD, (8E,12Z)-10-Hydroxy-8,12 octadecadienoic acid.

Next our specific goals is for the first time was to identify *M. javanica* effectors that alter plant fatty acid pathways and to functionally characterize interactions between nematode effectors and plant FA-related genes. During the second year the IS lab have completed a comprehensive RNA-seq of the nematode *Meloidogyne javanica*, the whole libraries which were generated and sequenced include the following a) biological duplicates of fresh hatched juveniles stage 2 (J2), with 17,117,546 reads; 2) biological duplicates of J2 exposed to protoplasts with 18,072,769 reads; 3) biological duplicates of J2 exposed to 13-KOD with 18,708,033 reads; 4) biological duplicates of J2 exposed to 9-HOT with 17,115,530 reads; 5) biological duplicates of J2 to MES buffer and ethanol with 17,734,243. The two libraries (fresh hatched juveniles and 9-HOT) which were not contaminated by plant, were assembled with the Trinity version 2.2.0 software for de novo assembly (assembly statistics N50 contigs). We mapped the different libraries to the two above mentioned references using Bowtie2 software, RSEM software was used for the quantification of RNAseq. EdgeR Bioconductor package was used for DEGs calculations and normalization of the count data.

We found accordingly 9376 DEGs in at least one of the treatment. The sequences were annotated by Trinotate software Version 3.0 and compared to BLAST against Swiss-prot protein database, nematode, uniref and compared to *Meloidogyne incognita*, *Meloidogyne hapla* and *Meloidogyne floridensis* from wormbase database, pearson correlation was calculated using R. Heat-map and clustering of the genes were visualized by using the hclust in R software. We used a threshold of $FDR < 0.0001$ and the criterion that expression level

increased or decreased by a factor greater or less than 2 on a logarithmic (base 2) scale (Fig. 11).

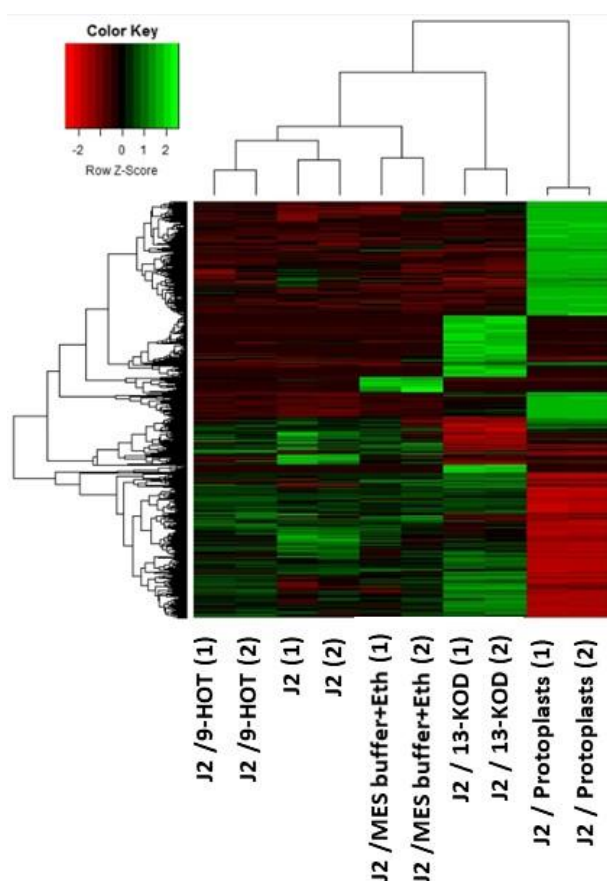


Figure 11. Heat-map diagram showing the differentially expressed genes of J2 exposed to 9-HOT, 13-KOD, protoplasts along with their controls. Heat map showing relative expression of 6335 differentially expressed genes. Color key represents normalized expression centered and log 2 scale.

Given that we were predominantly interested in genes that might be involved in parasitism i.e. effectors, the next step was to operate *in silico* analysis to identify differential transcripts which might be potential secreted effectors, For that purpose, DEGs which

include a predicted signal peptide according to SignalP4.1, were subjected to Venn diagram analysis illustrating DEGs distribution among treatments (Figure 12). A total of 728 DEGs included a signal peptide, whereas 310 DEGs showed significant matches in the NCBI database. A total of 519 DEGs (71.3%) were found to be expressed only by 9-HOT treatment, 61 DEGs (8.4%) were common between 9-HOT and the protoplasts treatments. A total of 143 DEGs (19.6%) were found to be expressed only by the protoplasts treatment and 5 DEGs (0.7%) were common between 9-HOT and 13-KOD treatments (Figure 12).

regulated by 9-HOT treatment were analyzed for GO-enriched profile using BLAST2go and Fisher's Exact Test. Among the 580 DEGs, 177 were annotated and showed an up-regulation

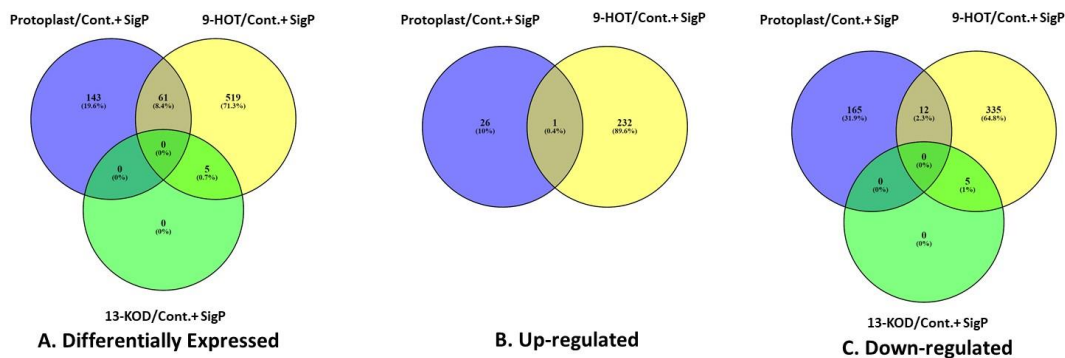


Figure 12. (A) Venn diagram showing the number of overlapping and non-overlapping *M. javanica*'s differentially expressed genes encoding signal peptide according to SignalP4.1 regulated (up- and down-regulated) exposed to different treatments: protoplasts/control, 9-HOT/control and 13-KOD/control. (B) Differentially expressed genes encoding signal peptide that were up-regulated. (C) Differentially expressed genes encoding signal peptide that are down-regulated (no down-regulated DEGs including a predicted signal peptide were found in 13-KOD/control treatment). Fold change with an absolute value >2 and P value ≤ 0.05 was used for the analyses.

induced by 9-HOT treatment. The included genes were involved in development such as MLT-10, several genes encoding cuticlin-1 and collagen, chitin synthase, astacin-like metalloendopeptidase. A group of genes implicate in oxidation-reduction activity and implicate in oxidative stress response were induced by 9-HOT (flavin-containing monooxygenase, gamma-glutamyltranspeptidase, glutaredoxin and thioredoxin-like domain, glutathione S-transferase-1). Secreted genes that might be associated with GC initiation (expansin, DNA replication licensing factor MCM2, inositol monophosphatase, Tonsoku-like protein, protein regulator of cytokinesis 1, SFRP-2) as well as genes encoding CWDE/CWME (lysosomal alpha-mannosidase-like, glycoside hydrolase) were found to be

up-regulated Moreover, genes involved in lipid modification (several genes of lipase, lipid binding, calycin domain and thioesterase) were also differentially expressed by 9-HOT treatment (BioProject Accession PRJNA480605). To confirm the

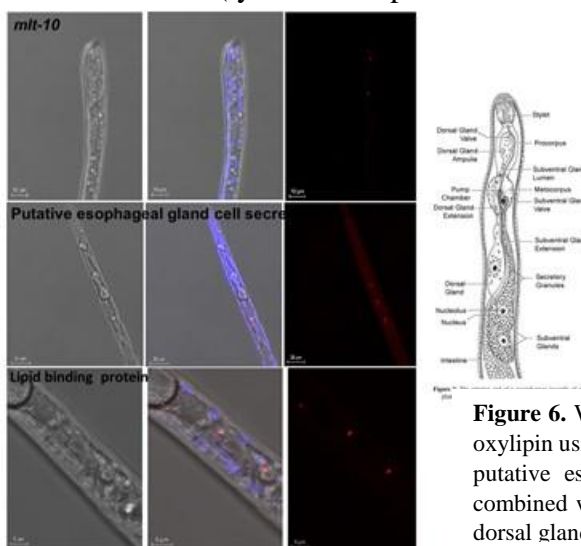


Figure 6. Whole-mount FISH analysis of infective J2s exposed to 9-HOT oxylin using confocal microscopy. Specific FISH probe (red) for Mlt-10, putative esophageal gland cell and lipid binding encoding transcripts combined with DAPI. Signals were detected within the subventral and/or dorsal glands only after J2 exposure to 9-HOT oxylin.

expression of candidate effectors upon 9-HOT oxylin application we performed FISH

(Fluorescent in situ hybridization) analysis (Fig. 13). Our results clearly show these effectors are localized within the secretory glands and are highly induced upon 9-HOT application (Fig. 13).

References

1. Baldacci-Cresp F, Chang C, Maucourt M, Deborde C, Hopkins J, et al. (Homo) glutathione deficiency impairs root-knot nematode development in *Medicago truncatula*. (2012) *PLoS Pathogens* 8: e1002471.
2. Eulgem T, Rushton PJ, Robatzek S, Somssich IE. The WRKY superfamily of plant transcription factors. (2000) *Trends in plant science* 5: 199-206.
3. Hok S, Danchin EG, Allasia V, Panabieres F, Attard A, et al. An Arabidopsis (malectin-like) leucine-rich repeat receptor-like kinase contributes to downy mildew disease. (2011) *Plant, cell & environment* 34: 1944-1957.
4. Iberkleid I, Sela N, Brown Miyara S. Meloidogyne javanica fatty acid- and retinol-binding protein (Mj-FAR-1) regulates expression of lipid-, cell wall-, stress- and phenylpropanoid-related genes during nematode infection of tomato. (2015) *BMC genomics* 16: 272.
5. Lee S-H, Ahsan N, Lee K-W, Kim D-H, Lee D-G, et al. Simultaneous overexpression of both CuZn superoxide dismutase and ascorbate peroxidase in transgenic tall fescue plants confers increased tolerance to a wide range of abiotic stresses. (2007) *Journal of plant physiology* 164: 1626-1638.
6. Marrs KA. The functions and regulation of glutathione S-transferases in plants. (1996) *Annual review of plant biology* 47: 127-158.
7. Pandey SP, Somssich IE. The Role of WRKY Transcription Factors in Plant Immunity. (2009) *Plant Physiology* 150: 1648-1655.
8. Rushton PJ, Somssich IE, Ringler P, Shen QJ. WRKY transcription factors. (2010) *Trends in plant science* 15: 247-258.
9. Wesley SV, Helliwell CA, Smith NA, Wang M, Rouse DT, et al. Construct design for efficient, effective and high-throughput gene silencing in plants. (2001) *The Plant Journal* 27: 581-590.

Changes in direction from that in the original proposal. The approaches of yeast two-hybrid screens targeting plant (LOX) proteins against 30 *M. incognita* effectors, or full root cDNA Y2H library screening against the same *M. incognita* effectors have been cumbersome and produced only one potential lead (Mi2G2-AtGST16 above) involved in lipid signaling within host plant cells. We have altered the approach in Year 3 to identify *M. incognita* effectors that alter plant host lipid-signaling pathways using a transient expression system in *N. benthamiana* leaves. This functional approach is more objective and provides the potential to identify more *M. incognita* effectors that affect host lipid signaling pathways than the direct protein-protein interaction approach above. In addition in order to identify potential effectors which are involve in regulating plant lipid signaling the RNAseq approach involved second stage juveniles J2s treated with 9-HOT and 13-KOD oxylipin as well as exposure to protoplasts. Altogether these experiments yielded a list of candidate effectors which were used for further research.

Publications for Project IS-4727-14R

Stat us	Type	Authors	Title	Journal	Vol:pg Year	Cou n
Published	Reviewed	<i>Chinnapandi Bharathiraja</i>	SIWRKY45, nematode-responsive tomato WRKY gene, enhances susceptibility to the root knot nematode; <i>M. javanica</i> infection	<i>Plant Signal Behaviour</i>	12(12) : 12(12):e1 356530 2017	IS only
Published	Abstract - Presentati on	<i>Sigal Braun Miyara</i>	PLANT-NEMATODE LIPIDOME: A TRANSCRIPYOMIC AND METABOLOMIC INSIGHT	<i>The American Society of Nematology</i>	: 2017	Joint
Published	Abstract - Presentati on	<i>Sigal Braun Miyara</i>	WRKYs transcription factors regulating <i>Solanum lycopersicum</i> response to root knot nematode: transcriptomic and metabolomics insights	<i>The American Society of Nematology</i>	: 2018	IS only
Published	Abstract - Presentati on	<i>Chinnapandi Bharathiraja</i>	WRKYs transcription factors regulating <i>Solanum lycopersicum</i> response to root knot nematodes: transcriptomic and metabolomics insights.	<i>European Society of Nematology</i>	: 2018	IS only
Published	Abstract - Presentati on	<i>Sigal Braun Miyara</i>	Lipid signals as part of plant –nematodes language	<i>Nematode Chemosensation workshop</i>	: 2017	IS only
Published	Book Chapter	<i>Sigal Braun Miyara</i>	The role of lipid signalling in regulating plant-nematode interactions	<i>Advances in Botanical Research</i>	: 2015	Joint